Supplemental material to this article can be found at:
http://molpharm.aspetjournals.org/content/suppl/2021/05/24/molpharm.120.000211.DC1
1521-0111/100/2/170–180$35.00 https://doi.org/10.1124/molpharm.120.000211
MOLECULAR PHARMACOLOGY Mol Pharmacol 100:170–180, August 2021

A20-Binding Inhibitor of Nuclear Factor-κB Targets β-Arrestin2 to Attenuate Opioid Tolerance[S]

Yixin Zhang, Peilan Zhou, Fengfeng Lu, Ruibin Su, and Zehui Gong

State Key Laboratory of Toxicology and Medical Countermeasures, Beijing Key Laboratory of Neuropsychopharmacology, Beijing Institute of Pharmacology and Toxicology, Beijing, China

Received November 23, 2020; accepted April 26, 2021

ABSTRACT

Opioids play an important role in pain relief, but repeated exposure results in tolerance and dependence. To make opioids more effective and useful, research in the field has focused on reducing the tolerance and dependence for chronic pain relief. Here, we showed the effect of A20-binding inhibitor of nuclear factor-κB (ABIN-1) in modulating morphine function. We used hot-plate tests and conditioned place preference (CPP) tests to show that overexpression of ABIN-1 in the mouse brain attenuated morphine dependence. These effects of ABIN-1 are most likely mediated through the formation of ABIN-1–β-arrestin2 complexes, which accelerate β-arrestin2 degradation by ubiquitination. With the degradation of β-arrestin2, ABIN-1 overexpression also decreased μ opioid receptor (MOR) phosphorylation and internalization after opioid treatment, affecting the β-arrestin2–dependent signaling pathway to regulate morphine tolerance. Importantly, the effect of ABIN-1 on morphine tolerance was abolished in β-arrestin2–knockout mice. Taken together, these results suggest that the interaction between ABIN-1 and β-arrestin2 inhibits MOR internalization to attenuate morphine tolerance, revealing a novel mechanism for MOR regulation. Hence, ABIN-1 may be a therapeutic target to regulate MOR internalization, thus providing a foundation for a novel treatment strategy for alleviating morphine tolerance and dependence.

SIGNIFICANCE STATEMENT

A20-binding inhibitor of nuclear factor-κB (ABIN-1) overexpression in the mouse brain attenuated morphine tolerance and dependence. The likely mechanism for this finding is that ABIN-1–β-arrestin2 complex formation facilitated β-arrestin2 degradation by ubiquitination. ABIN-1 targeted β-arrestin2 to regulate morphine tolerance. Therefore, the enhancement of ABIN-1 is an important strategy to prevent morphine tolerance and dependence.

Introduction

Opioids, such as morphine, have powerful analgesic effects and are used to relieve acute and chronic pain; however, their repeated or continuous use can result in tolerance and dependence issues. These effects limit the clinical utility of morphine as an analgesic. Opioids act on μ opioid receptor (MOR) to activate G protein–dependent and β-arrestin–mediated signaling (Whalen et al., 2011; Williams et al., 2013). Although superactivation or sensitization of adenylate cyclase by chronic agonist treatment in the G protein–dependent signaling pathway is considered the classic mechanism of opioid tolerance (Sharma, 1975), β-arrestin–mediated signaling has also been shown to play an important role in morphine tolerance (Bohn et al., 1999; Bohn et al., 2000; Li et al., 2009; Whalen et al., 2011; Williams et al., 2013; Allouche et al., 2014; Kliewer et al., 2019).

β-Arrestins, including β-arrestin1 and β-arrestin2, are highly expressed in the central nervous system and play critical roles in regulating MOR function (Attramadal et al., 1992; Le Rouzic et al., 2019). Several lines of evidence suggest that β-arrestin expression, especially that of β-arrestin2, is involved in the internalization of MOR. In mouse embryonic fibroblasts, β-arrestin2 is recruited after MOR phosphorylation, which causes a sequestration of MOR after morphine exposure (Groer et al., 2011). In addition, ubiquitinated β-arrestins are crucial for downstream endocytic and signaling processes (Takenouchi et al., 2018). Mice lacking β-arrestin2 did not develop tolerance in a hot-plate test after chronic morphine treatment, suggesting the vital role β-arrestin2 plays in MOR regulation (Sadat-Shirazi et al., 2019). Several proteins mediate morphine tolerance by regulating β-arrestin2. For example, TRPV1 promoted rapid translocation of β-arrestin2 to the nucleus and decreased the desensitization of MOR, which in turn enhanced the analgesic effect (Basso et al., 2019). Likewise, the vasopressin 1b receptor enhanced morphine analgesia by modulating the interaction between β-arrestin2 and MOR (Koshimizu et al., 2018). Additionally, MiR-365–mediated downregulation of β-arrestin2 reduced the antinociceptive tolerance to morphine

This work was supported by the National Natural Science Foundation of China [Grant 81473194].
The authors declare that they have no competing interests.
https://dx.doi.org/10.1124/molpharm.120.000211.
[S] This article has supplemental material available at molpharm.aspetjournals.org.

ABBREVIATIONS: ABIN-1, A20-binding inhibitor of nuclear factor-κB; ARRB2$^{-/-}$, β-arrestin2–knockout; AUC, area under the curve; CPP, conditioned place preference; DAMGO, [D-Ala2, *N*-MePhe4, Gly-ol]-enkephalin; ERK, extracellular regulated protein kinase; HEK293, human embryonic kidney 293; MAPK, mitogen-activated protein kinase; MOR: μ opioid receptor; %MPE, percentage of the maximal possible effect; N2A, Neuro-2A; phos-, phosphorylated; sh, short hairpin; WT, wild type.

(Wu et al., 2018). Recently, MOR-associated proteins that negatively regulate the β-arrestin2 signaling pathway are being considered as therapeutic targets and molecular probes to resolve issues regarding chronic opioid use. Notably, studies have shown the feasibility and potential clinical utility of biased MOR agonists, such as PZM21 and TRV130 (Manglik et al., 2016).

A20-binding inhibitor of nuclear factor-κB (ABIN-1) is well known as a ubiquitin-binding protein that plays an important role in autoimmune inflammatory diseases, such as systemic lupus erythematosus and psoriasis, by its inhibitory action on nuclear factor-κB activation (Heyninck et al., 2003; Nanda et al., 2011). ABIN-1 has also been shown to bind to extracellular regulated protein kinase (ERK) 2 and suppress ERK2 entering into the nucleus (Zhang et al., 2002). In our previous study, we found that ABIN-1 functionally interacted with MOR and was upregulated in morphine-tolerant mice; ABIN-1 negatively regulated MOR function after acute opioid treatment in cell culture and zebrafish (Zhou et al., 2015; Zhou et al., 2018). However, the effect of ABIN-1 on the mouse after chronic opioid treatment is not clear. Thus, further studies should focus on determining the mechanism of ABIN-1 actions on morphine tolerance and dependence.

In the current study, we discovered that ABIN-1 in the mouse brain attenuated morphine dependence and tolerance. The interaction between ABIN-1 and β-arrestin2 increased the ubiquitination of β-arrestin2, which led to the degradation of β-arrestin2 and the reduction of MOR internalization. Additionally, we found that ABIN-1 overexpression or knockdown in β-arrestin2–knockout mice did not affect morphine antinociceptive tolerance. Overall, our results show a mechanism by which ABIN-1 acts on β-arrestin2 to regulate morphine tolerance.

Materials and Methods

Animals

We used C57BL/6J mice aged 8 weeks (18–22 g) for all the experiments in our study. The hot-plate test was conducted on the female mice, and the conditioned place preference (CPP) test was conducted on the male mice. Female β-arrestin2–knockout ($ARRB2^{-/-}$) mice obtained from the laboratory of R.J. Lefkowitz (Duke University Medical Center, Durham, NC) were backcrossed onto a C57BL/6J background. All animals were housed under temperature- and humidity-controlled conditions on a 12-hour light/12-hour dark cycle with free access to food and water. Animals were assigned into different treatment groups in a random manner. The experimental procedures were reviewed and approved by the Ethics Committee and Institutional Animal Care and Use Committee of Beijing Institute of Pharmacology and Toxicology, Beijing, China (IACUC of AMMS–06–2018–020). All efforts were made to minimize suffering and reduce the number of animals used.

Reagents

[D-Ala2, *N*-MePhe4, Gly-ol]-enkephalin (DAMGO) and naloxone were obtained from Sigma-Aldrich, and morphine hydrochloride was obtained from Qinghai Pharmaceutical Factory.

Behavioral Tests

Viral Constructs and Stereotaxic Microinjection. AAV2/9 viral vectors were designed and constructed using standard methods with assistance from BrainVTA (Wuhan, China). rAAV-CMV-ABIN-1-EGFP-WPRE-pA (AAV/PHPeB, titer: $\geq 3.00E^{+12}$ vg/ml) and rAAV-U6-shRNA (ABIN-1)-CMV-EGFP-pA (AAV/PHPeB, titer: $\geq 5.00E^{+12}$ vg/ml) were administrated through intracerebroventricular injection in the brain. C57BL/6J mice were anesthetized using xyz for stereotaxic viral injections. Viruses were unilaterally injected into the right cerebral ventricle (anteroposterior = −0.6 mm, mediolateral = 1.5 mm, dorsoventral = 2.0 mm, 5 μl, 0.5 μl/min).

Hot-Plate Test. Morphine (10 mg/kg, s.c.) antinociception was assessed according to a protocol described in the literature (Eddy and Leimbach, 1953). Female mice were placed on the surface of the hot-plate (55°C). The latency to jump and lick the hind paws was recorded from the start time for each mouse. A cutoff time of 60 seconds was used to prevent the possibility of tissue damage. Antinociceptive data are presented as a percentage of the maximal possible effect (%MPE) calculated by the following formula: %MPE = (post-drug latency – predrug latency)/(60 – predrug latency) × 100%.

Naloxone-Precipitated Withdrawal. Mice were administered morphine (10 mg/kg, s.c., twice daily) for 7 days. The antinociception effect of morphine was detected in the morning from day 1 to day 7. On day 7, mice were administrated naloxone (10 mg/kg, i.p.) 2 hours after the last injection of morphine and then individually placed in Plexiglas boxes (60 cm × 20 cm × 20 cm) for observation of the withdrawal signs, jumping, wet-dog shaking, and paw tremor, for 15 minutes.

Conditioned Place Preference Test. We assessed psychologic dependence on morphine in our mice using a morphine CPP test. The CPP test was performed using an unbiased, counterbalanced protocol (Wang et al., 2008). The CPP apparatus contained eight identical three-chamber polyvinyl chloride boxes (Lu et al., 2011). The two large compartments were different, with white walls and a bare floor in one compartment and black walls with a gridded floor in the second compartment, which provided distinct context pairing with morphine and saline administration. The three compartments were connected by manual guillotine doors. The CPP test paradigm is outlined in Fig. 1D. During the preconditioning period (from day 1 to day 3), male mice were free to move in all chambers of the apparatus for 15 minutes. The time spent by the mice in each chamber was recorded (AniLab v3.0, AniLab Software & Instrument Co. Ltd., Ningbo, China). Mice that showed a strong unconditioned preference (more than 540 seconds) for either compartment were excluded from the experiment such that our sample mouse population did not have an innate preference for one chamber. Mice underwent conditioning training (day 4 to day 8) for 5 days. During the conditioning phase, mice were administered normal saline (10 ml/kg, i.p.) in the morning and morphine (10 mg/kg, s.c.) in the afternoon, and this was followed by 30 minutes of training. The CPP test was conducted on the 9th day. The CPP score was calculated as the time (in seconds) spent in the drug-paired chamber after conditioning minus the time spent in the drug-paired chamber before conditioning.

Locomotor Activity. We used the LabState video tracking system (Anilab Scientific Instruments Co., Ltd., China) to measure spontaneous locomotor activity. The mice were placed in acrylic boxes (40 cm × 40 cm × 35 cm) for 30 minutes before morphine treatment on day 1. Mice were habituated for 1 hour before being placed in an open field. The locomotor activity of each mouse was defined by the horizontal distance it traveled (in centimeters) over 30 minutes.

Cell Culture and Transfection Conditions. Human embryonic kidney 293 (HEK293) cells were cultured in Dulbecco's modified Eagle's medium (Thermo Fisher Scientific) containing 10% FBS (v/v, Sigma-Aldrich). CHO cells stably expressing Flag-MOR (MOR-CHO) were grown in F12 (Thermo Fisher Scientific) medium containing 10% FBS and supplemented with G418 (200 μg/ml) (Thermo Fisher Scientific). CHO cells stably expressing Flag-MOR and Myc-ABIN-1 (MOR-ABIN-1-CHO) were grown in F12 medium containing 10% FBS and supplemented with G418 (200 μg/ml) and hygromycin B (200 μg/ml). Neuro-2A (N2A) cells were grown in Dulbecco's modified Eagle's medium containing 10% FBS. All cells were cultured at 37°C

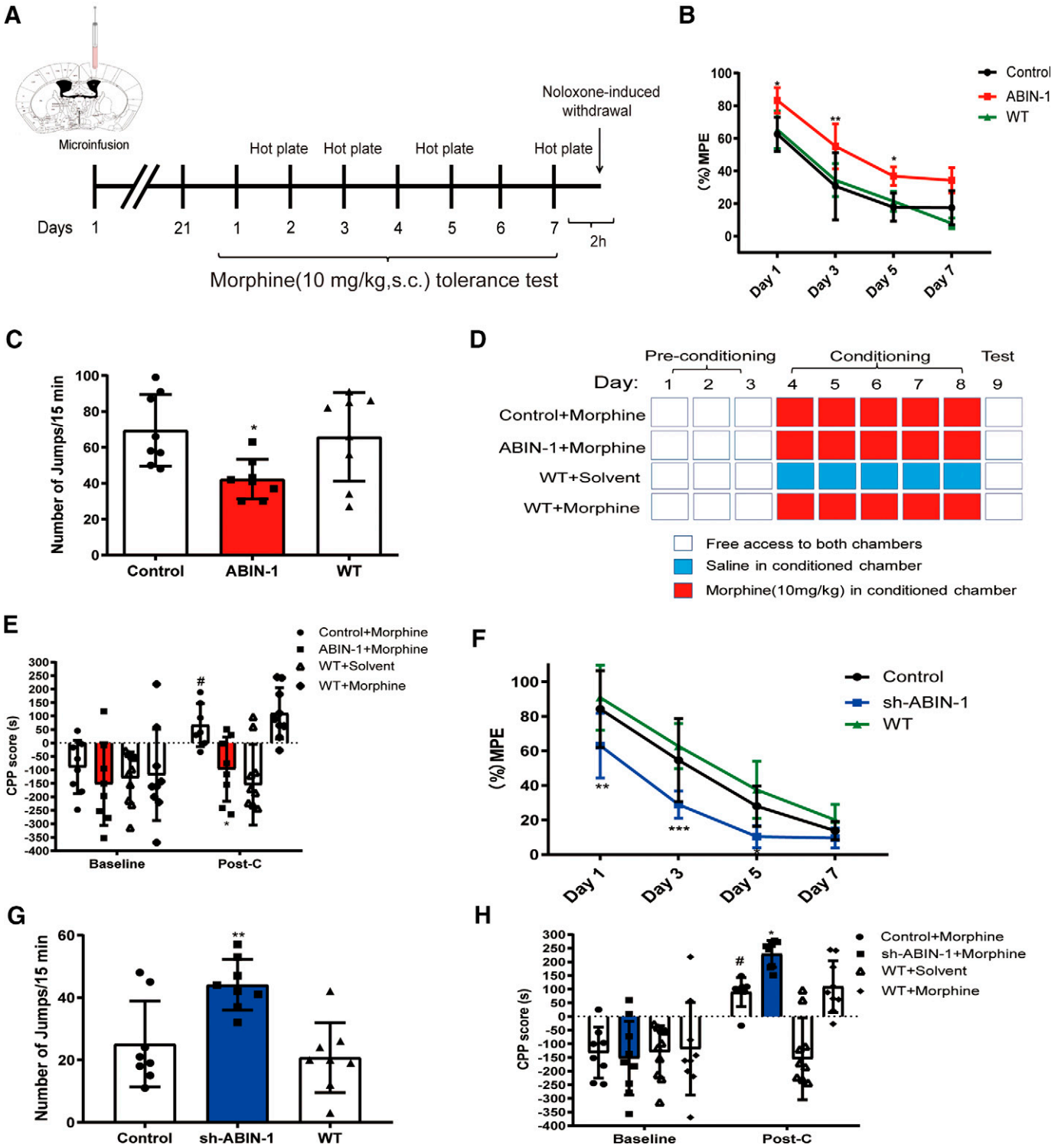

Fig. 1. ABIN-1 in brain decreased morphine tolerance and dependence. (A) Schematic of the experimental paradigm for the morphine-induced tolerance and naloxone-induced withdrawal test. (B, F) The %MPE of morphine analgesia after ABIN-1 overexpression (B, red lines) or knockdown (F, blue lines) in mice brains. (C, G) The naloxone-induced jumping counts after ABIN-1 overexpression (C, red bars) or knockdown (G, blue bars) in mice brains. (D) Schematic of experimental paradigm for morphine-induced CPP test. (E, H) CPP score after ABIN-1 overexpression (E) or knockdown (H) in mice brains. The error bars indicate the mean ± S.D.; the %MPE and CPP score results were analyzed by two-way ANOVA followed by Bonferroni post hoc test; the jumping counts were analyzed by one-way ANOVA followed by Bonferroni post hoc tests; $^{*}P < 0.05$, $^{**}P < 0.01$,$^{***}P < 0.001$, ABIN-1 vs. control; $\#\#P < 0.01$, postconditioning (Post-C) vs. baseline; hot-plate assay used female mice, $n = 8$; withdrawal assay used female mice, $n = 8$; CPP test used male mice, $n = 7$–8.

in a humidified atmosphere at 5% CO_2. Transient transfections were carried out using LipofectAMINE 3000 (Invitrogen) with cells grown to 65%–85% confluency.

Coimmunoprecipitation. HEK293 cells in 10-cm dishes were cotransfected with the plasmid using LipofectAMINE 3000 for 48 hours. Next, the cells were lysed immediately with EBC buffer [50

mM Tris-HCl (pH 8.0), 120 mM NaCl, 0.5% NP-40, and 1 mM EDTA] and a protease inhibitor mixture (Roche Applied Science) for 30 minutes on ice. The cells were centrifuged at 14,000 × *g* at 4°C for 20 minutes. The supernatant was divided into three parts; one part was denatured by incubation in boiling water for 10 minutes. The remaining supernatant was divided into two parts: 1 μg of anti-Flag antibody was added to one part, and 1 μg of IgG with the same properties was added to the other part. Both were kept on a shaker at 4°C overnight. Then, 30 μl of protein G magnetic beads (Thermo Fisher Scientific, Cat#88847) was added for 2 hours at 4°C. After three washes with EBC buffer, the protein was eluted with 50 μl of 1× SDS sample buffer for 10 minutes at 95°C.

Phosphorylation of MOR and ERK. MOR-CHO and MOR-ABIN-1-CHO cells were serum-starved for 2 hours prior to drug treatment. Cells were treated with DAMGO for 0 minutes, 5 minutes, 30 minutes, 60 minutes, 6 hours, 24 hours, 48 hours, and 72 hours and then lysed with lysis buffer [50 mM Tris-HCl (pH 7.4), 150 mM NaCl, 5 mM EDTA, 10 mM NaF, 10 mM disodium pyrophosphate, 1% Nonidet P-40, 0.5% sodium deoxycholate, protease inhibitor mixture, and 0.1% SDS]; they were then treated with phosSTOP phosphatase inhibitor (Roche) on ice for 30 minutes. The lysate was centrifuged at 14,000 × *g* for 20 minutes at 4°C. The supernatant was separated by SDS-PAGE, and immunoblot analysis was performed using anti–phos-MOR or anti–phos-ERK.

***β*-Arrestin2 Ubiquitination Assay.** pcDNA3.1myc-hisB-ABIN-1, pCMV-Flag-*β*-arrestin2, and pcDNA3.1-MOR were transiently transfected into HEK293 cells for 24 hours. Cells were serum-starved for at least 2 hours and then stimulated with DAMGO for 30 minutes. Next, cells were solubilized in lysis buffer [50 mM Tris-HCl (pH 8.0), 150 mM NaCl, 5 mM EDTA, 0.1% SDS, 10% glycerol, 1% Nonidet P-40, 0.5% deoxycholate, 10 mM sodium orthovanadate, 10 mM NaF, and 10 mM *N*-ethylmaleimide] with a protease inhibitor mixture. Cell lysates were mixed with FLAG M2 affinity beads (Sigma-Aldrich) and rotated at 4°C overnight. The precipitate was washed three times in lysis buffer, and the protein was eluted with 50 μl of 2× loading buffer and analyzed by SDS-PAGE.

Internalization of MOR. The plasma membrane protein fraction of both cells and brain tissue was separated by a plasma membrane protein isolation kit (Invent Biotechnologies) to determine the internalization of MOR. Cells or tissue in buffer A were placed on ice for 5–10 minutes and were then centrifuged at 16,000 × *g* for 30 seconds. The supernatant was discarded, and the pellet was resuspended by vigorous vortexing for 10 seconds. The resulting suspension was centrifuged at 700 × *g* for 1 minute. The supernatant was transferred to a fresh 1.5-ml microcentrifuge tube and centrifuged at 16,000 × *g* for 30 minutes at 4°C. The supernatant was removed, and the pellet (the total membrane protein fraction including organelles and plasma membranes) was retained. The total membrane protein fraction was resuspended in 200 μl of buffer B by repeatedly pipetting up and down or vortexing. The resulting suspension was centrifuged at 7,800 × *g* for 5 minutes at 4°C, and the supernatant was removed. Ice-cold PBS (1.6 ml) was added and centrifuged at 16,000 × *g* for 30 minutes at 4°C. The isolated plasma membrane proteins in the pellet were retained and then separated by SDS-PAGE.

Confocal Immunofluorescence. HEK293 cells were seeded into 35-mm cell culture dishes with coverslips attached and then transfected with pcDNA3.1myc-hisB-ABIN-1 and pEGFP-N3-*β*-arrestin2 using LipofectAMINE 3000, as mentioned above. Immunocytochemistry was performed as previously described (Zhou et al., 2015). Next, cells were fixed with 4% paraformaldehyde for 30 minutes, after which the fixed solution was aspirated and washed three times with PBS for 3 minutes each time. These cells were then incubated in 0.5% Triton X-100 in PBS for 20 minutes at room temperature and washed three times in 1× PBS. Cells were blocked for 30 minutes (1% bovine serum albumin), washed with PBST, incubated with the primary anti-myc antibody (Abcam, 1:200) at 4°C overnight, and washed three times in 1× PBST. Finally, the cells were incubated with rhodamine-conjugated Affinipure goat anti-mouse IgG antibody (1:100; Santa Cruz) for 1 hour at room temperature. Cells were then washed and treated with DAPI Fluoromount-GTM (VECTOR) for 5 minutes at room temperature in the dark and then mounted onto glass slides. The cells were examined using a laser-scanning Zeiss LSM510 confocal microscope.

Statistical Analysis. Statistical analyses were performed using GraphPad Prism 7.0 software (GraphPad Software Inc., La Jolla, CA). The results are expressed as the mean ± S.D. The effect of ABIN-1 viral vector injection in the brain or the cell assay was analyzed using two-way ANOVA followed by the Bonferroni post hoc test. The naloxone precipitation test was analyzed using one-way ANOVA followed by the Bonferroni post hoc test. The criterion for statistical significance was set at $P < 0.05$ for all analyses.

Results

ABIN-1 Attenuates Morphine-Induced Tolerance and Dependence. To investigate the role of ABIN-1 in morphine-induced tolerance and dependence, we infused rAAV(PHPeB)-ABIN-1 by intracerebroventricular injection to upregulate ABIN-1 levels in the mouse brain. The antinociception induced by morphine was assessed by hot-plate test 21 days after viral infusion [rAAV(PHPeB)-vector (control), rAAV(PHPeB)-ABIN-1] in mice and wild-type (WT) mice (Fig. 1A). ABIN-1 was overexpressed in the central nervous system, specifically in the hippocampus, as observed via immunoblot analysis and immunofluorescence (Supplemental Fig. 1A). Prior to morphine treatment, the locomotor behavior of the mice was similar among the three groups of mice (Supplemental Fig. 1D), and the basal nociceptive latencies in the ABIN-1 overexpression group were also similar to those of control and WT from days 1 to 7 (Supplemental Fig. 1E).

The %MPE of the ABIN-1 upregulated group decreased gradually after chronic morphine treatment (10 mg/kg, s.c.). However, the %MPE differed between the control group and ABIN-1 upregulated group after morphine treatment. The %MPE in the ABIN-1 overexpression group was higher than the control group after morphine exposure on days 1, 3, and 5 (day 1: $P = 0.0194$, day 3: $P = 0.0051$, day 5: $P = 0.0325$; $F(1, 7) = 71.75$, $P < 0.0001$; Fig. 1B). The area under curve (AUC) was calculated by hot-plate test data and used as the quantitative indicator for antinociceptive effects of drugs. ABIN-1 overexpression augmented the value of AUC, showing that ABIN-1 increased morphine analgesia with a decreased morphine tolerance after chronic morphine treatment (ABIN-1 vs. control; 150.6 ± 11.86 vs. 88.38 ± 17.45). We also analyzed naloxone-induced (10 mg/kg, i.p.) withdrawal response after chronic morphine treatment. Similar to inhibition of morphine-induced antinociceptive tolerance by ABIN-1 overexpression, ABIN-1 decreased naloxone-precipitated jumping behavior, the most sensitive and reliable index of withdrawal related to physical dependence on morphine (el-Kadi and Sharif, 1994) ($P = 0.0212$; Fig. 1C) but had no effect on paw tremor and wet-dog shaking (Supplemental Fig. 1H). To investigate whether ABIN-1 would affect the psychologic dependence on morphine, the CPP test was conducted in four groups of mice with viral infusion (as mentioned above) as well as in WT mice (with solvent, morphine addition) (Fig. 1D). The baseline CPP score between the ABIN-1 overexpression group and the control group was not different statistically. After 5 days of conditioning, the mice in the control group as well as in the WT group showed a clear preference for the morphine-paired compartment ($P = 0.0414$). In contrast, mice in the ABIN-1 overexpression group did not prefer the white box.

The CPP was inhibited in ABIN-1 overexpression mice in comparison with the control group ($P = 0.0159$; Fig. 1E). The mice with solvent treatment also preferred the black compartments without CPP.

Next, we tested antinociception tolerance as well as physical and psychologic dependence induced by morphine treatment on ABIN-1 knockdown mice. ABIN-1 was downregulated by microinfusion of rAAV(PHPeB)-ABIN-1-shRNA in the brain (Supp1emental Fig. 1C). Prior to morphine treatment, the mice locomotor behavior on day 1 and nociceptive latencies from days 1 to 7 in the ABIN-1 knockdown group, the control, and the WT group were similar (Supplemental Fig. 1, F and G). Compared with the control group, the %MPE in the ABIN-1 knockdown group was decreased after morphine administration on days 1, 3, and 5 (day 1: $P = 0.0032$, day 3: $P = 0.0004$, day 5: $P = 0.0156$, $F(1, 7) = 15.39$, $P < 0.0044$; Fig. 1F). Similar to the AUC result for ABIN-1 overexpression, ABIN-1 knockdown decreased the AUC to reduce morphine analgesia after chronic morphine treatment (sh-ABIN-1 vs. control; 75.61 ± 12.01 vs. 131.6 ± 22.02). The antinociception in the control group had no obvious difference from the WT group after morphine chronic addition. In the naloxone withdrawal test, there was an augmentation in jumping behavior ($P = 0.0059$; Fig. 1G) and wet-dog shaking ($P = 0.0107$; Supplemental Fig. 1I) in the mice precipitated by naloxone in the ABIN-1 knockdown group compared with the control group, but ABIN-1 knockdown had no effect on paw tremor (Supplemental Fig. 1I). To confirm the role of ABIN-1 in morphine analgesia, we used AAV-ABIN-1-shRNA to decrease ABIN-1 expression in mice brains for 2 weeks and then reversed expression of ABIN-1 by AAV-ABIN-1 for 2 weeks. After restoration of ABIN-1 expression in ABIN-1 knockdown mice, the effect of ABIN-1 knockdown on morphine analgesia was blocked, and the mice almost recovered similar to the WT mice, demonstrating ABIN-1 expression in mice brains is involved in morphine analgesia (day 1: $P = 0.0146$, day 3: $P = 0.1071$, day 5: $P = 0.0078$, day 7: $P = 0.2930$, $F(1, 8) = 11.94$, $P = 0.0086$; Supplemental Fig. 2). In the CPP test, as seen in the previous experiment, the mice in the control group showed a clear preference for the morphine-paired compartment after 5 days of conditioned training ($P = 0.035$). Importantly, compared with the control group, the CPP score in the ABIN-1 downregulated group was higher than the score in the control group ($P = 0.0302$; Fig. 1H). Taken together, these results suggested that ABIN-1 in the brain attenuated antinociceptive tolerance and dependence induced by morphine treatment.

ABIN-1 Promotes β-Arrestin2 Ubiquitination and Degradation by Protein Interaction. Previous studies have shown that β-arrestin2 plays an important role in morphine tolerance (Bohn et al., 2000, 2002); thus, we suspected that ABIN-1 may affect morphine tolerance through β-arrestin2. Therefore, we explored the relationship between ABIN-1 and β-arrestin2. First, the interaction between ABIN-1 and β-arrestin2 was determined by immunofluorescence and coimmunoprecipitation experiments in HEK293 cells. Confocal microscopy revealed that myc-tagged ABIN-1 and GFP–β-arrestin2 were predominantly distributed in the cytoplasm close to the membrane in HEK293 cells. Because of the coexpression of the two proteins, ABIN-1 and β-arrestin2 overlapped, as displayed by the orange color in HEK293 cells (Fig. 2A). We found that there was a strong correlation between ABIN-1 and β-arrestin2 ($R = 0.74$) in HEK293 cells. The association between ABIN-1 and β-arrestin2 was further investigated by coimmunoprecipitation. β-Arrestin2 was immunoprecipitated using a monoclonal anti-Flag antibody from the lysate of HEK293 cells transiently cotransfected with pcDNA3.1-myc-hisB-ABIN-1 (with transfection of pcDNA3.1-myc-hisB in control group), pCMV-Flag-β-arrestin2 (with pCMV-Flag in control cells), and pcDNA3.1-MOR. The immunoprecipitate was immunoblotted with antibodies against ABIN-1. ABIN-1 was found in the immunoprecipitate from cells that coexpressed ABIN-1 and β-arrestin2 (Fig. 2B). The interaction of ABIN-1 and β-arrestin2 increased after DAMGO (10 μM) treatment. The interaction of the ABIN-1 and β-arrestin2 was also studied in N2A cells, which have endogenous ABIN-1 and β-arrestin2 proteins. As shown in Fig. 2C, β-arrestin2 was immunoprecipitated from the lysate of N2A cells using anti–β-arrestin2 antibodies. The immunoprecipitate was immunoblotted with antibodies against ABIN-1. ABIN-1 was found to interact with β-arrestin2 by coimmunoprecipitation. Then, β-arrestin2 ubiquitination was analyzed by coimmunoprecipitation in the HEK293 cells as mentioned above. In comparison with the control group, ubiquitination of β-arrestin2 was upregulated by ABIN-1 overexpression with or without DAMGO (10 μM) treatment (0 minutes: $P = 0.0078$, 30 minutes: $P = 0.0361$, $F(1, 4) = 20.81$, $P = 0.0103$; Fig. 2D). Ubiquitin was originally identified as a tag for protein degradation. We measured the effect of ABIN-1 overexpression on β-arrestin2 levels in the N2A cell lines that had stable expression of β-arrestin2. ABIN-1 was overexpressed in N2A cells by transient transfection with pcDNA3.1-myc-hisB-ABIN-1 (with pcDNA3.1-myc-hisB as control). We found that β-arrestin2 was notably decreased with or without treatment with DAMGO for 30 minutes (10 μM) compared with its level in control cells (0 minutes: $P = 0.0122$, 30 minutes: $P = 0.0444$, $F(1, 4) = 40.44$, $P = 0.0031$; Fig. 2E). These data suggested that ABIN-1 decreased β-arrestin2 expression by interaction.

ABIN-1 Decreases the Phosphorylation and Internalization of MOR. β-Arrestin2 is associated with MOR phosphorylation and internalization (Shukla et al., 2011). We investigated the level of MOR phosphorylation at Ser375 (Schulz et al., 2004) (phos-MOR) after acute and chronic opioid treatment. We noted that in MOR-CHO cells, the phosphorylation of MOR increased after DAMGO (10 μM) treatment of 5 minutes followed by a decrease in the phosphorylation after 30 and 60 minutes of treatment. However, in MOR-ABIN-1-CHO cells, the increase in MOR phosphorylation was inhibited after DAMGO (10 μM) treatment at 5, 30, and 60 minutes compared with the MOR phosphorylation in MOR-CHO cells (0 minutes: $P > 0.9999$, 5 minutes: $P = 0.0064$, 30 minutes: $P = 0.4320$, 60 minutes: $P = 0.0465$, $F(1, 2) = 11.34$, $P = 0.0780$; Fig. 3A). After 24 to 72 hours of DAMGO treatment, MOR phosphorylation was upregulated in MOR-CHO cells. In contrast, MOR phosphorylation decreased with ABIN-1 overexpression in MOR-ABIN-1-CHO cells after chronic DAMGO exposure for 24 to 72 hours in comparison with its phosphorylation in MOR-CHO cells (0 minutes: $P > 0.9999$, 5 minutes: $P = 0.0222$, 24 hours: $P = 0.0124$, 48 hours: $P = 0.0068$, 72 hours: $P = 0.0012$, $F(1, 2) = 43.54$, $P = 0.0222$; Fig. 3B).

Studies have shown that phosphorylated MOR recruits β-arrestin2 to the plasma membrane, which triggers the internalization of MOR (Groer et al., 2011). We extracted MOR in the membrane from MOR-CHO and MOR-ABIN-1 CHO cells. In MOR-CHO cells, the MOR in the membrane was decreased after acute (0 minutes: MOR-CHO vs. 30

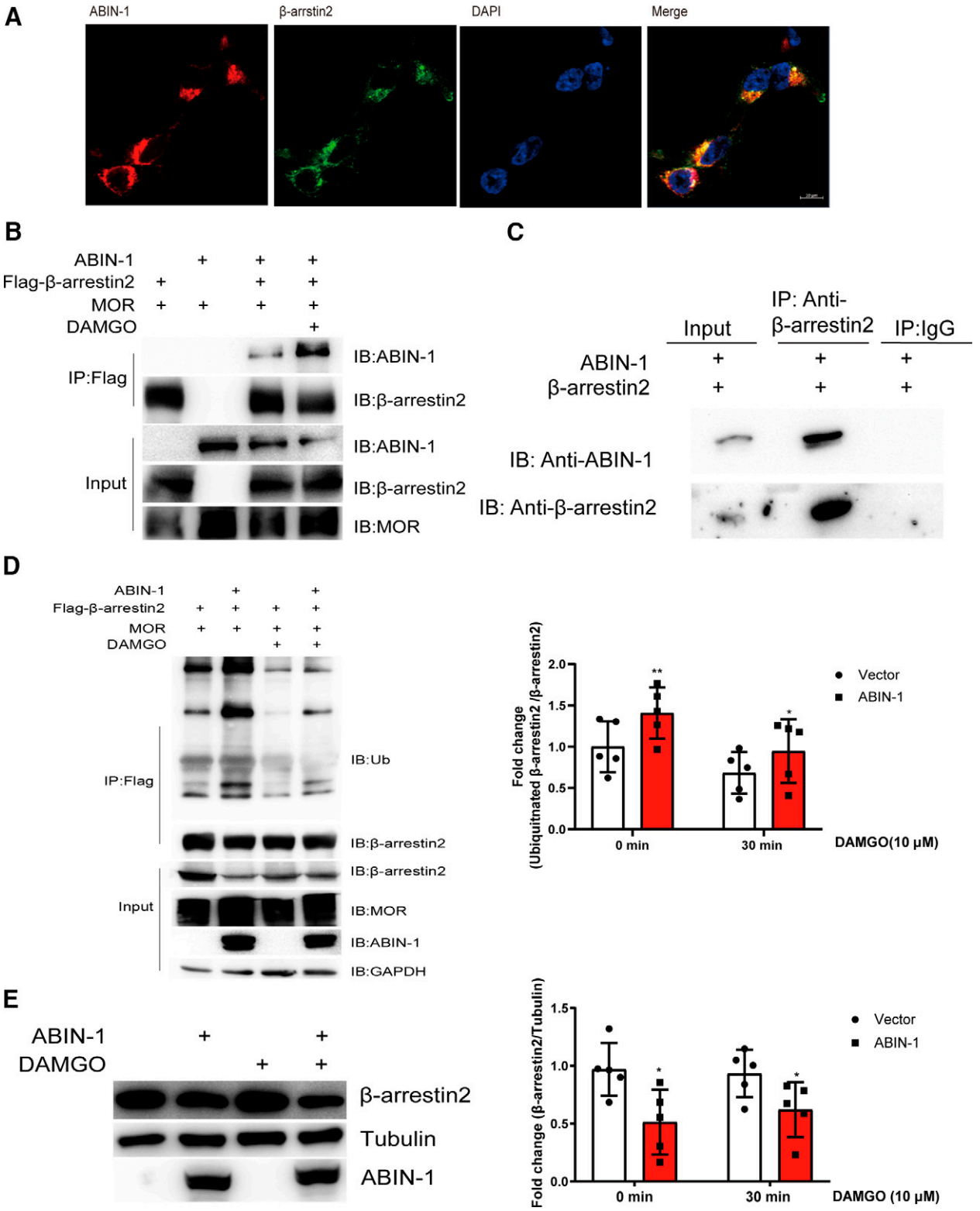

Fig. 2. ABIN-1 interacts with β-arrestin2 and promotes β-arrestin2 ubiquitination and degradation. (A) Colocalization of ABIN-1 (red) and β-arrestin2 (green) in HEK293 cells. Bar, 10 μm, Pearson's R value: 0.74. The confocal microscopic images are representative results from three independent experiments. (B) Immunoblot analysis showing the interaction between ABIN-1 and β-arrestin2 with or without DAMGO (10 μM) treatment using coimmunoprecipitation. (C) Immunoblot analysis showing the interaction between ABIN-1 and β-arrestin2 in Neuro 2A cells using coimmunoprecipitation. (D) Immunoblot analysis showing the ubiquitination of β-arrestin2 in HEK293 cells with ABIN-1 and MOR overexpression under DAMGO (10 μM) treatment after coimmunoprecipitation. (E) Immunoblot analysis showing levels of β-arrestin2 in Neuro-2A cells with overexpressed ABIN-1 after DAMGO (10 μM) treatment. The error bars indicate the mean ± S.D., two-way ANOVA followed by Bonferroni post hoc test, $^{*}P < 0.05$, $^{**}P < 0.01$, ABIN-1 vs. vector, $n = 5$.

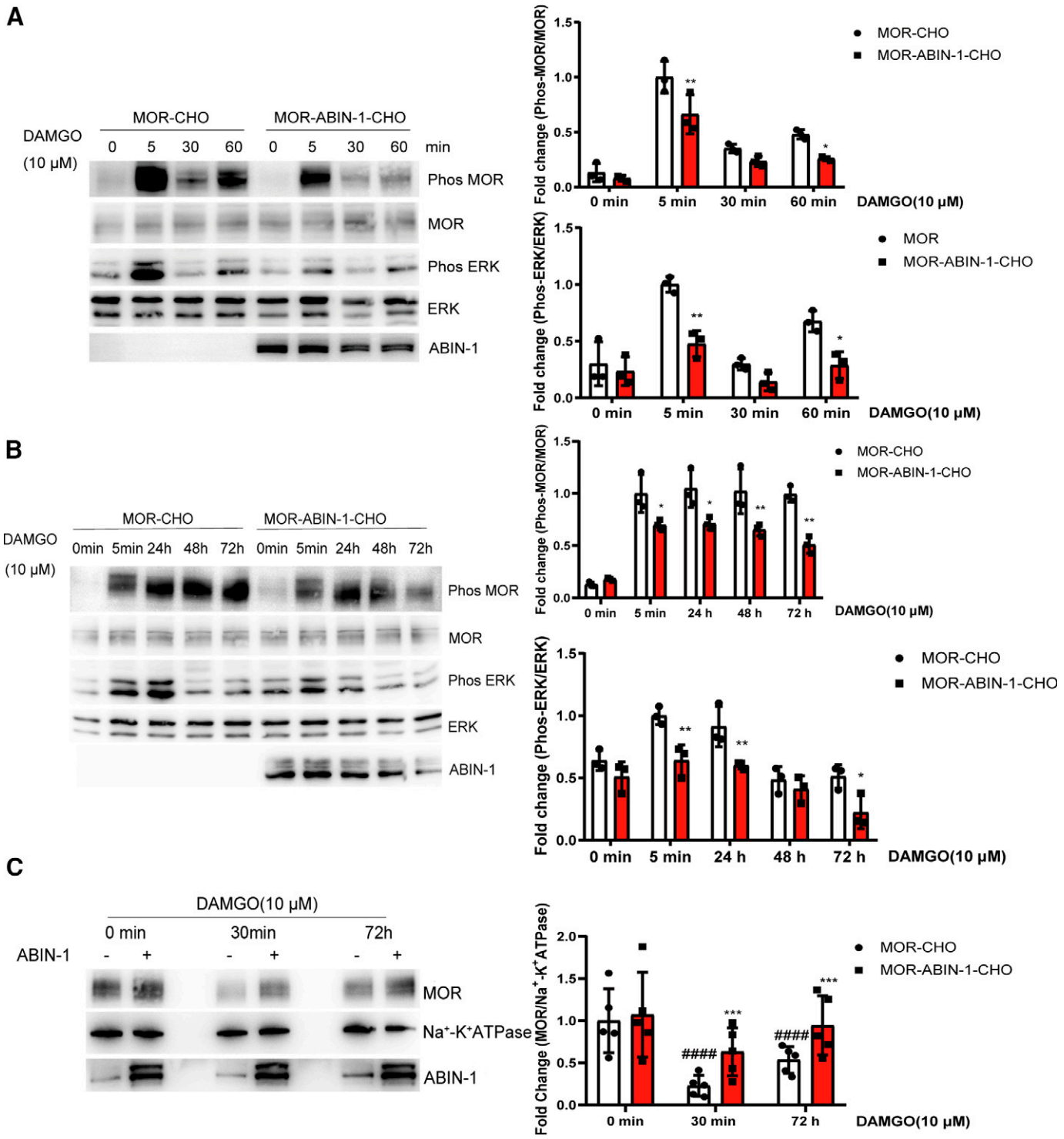

Fig. 3. ABIN-1 inhibits the phosphorylation and internalization of MOR. (A and B) Immunoblot analysis showing levels of phos-MOR and phos-ERK in MOR-CHO and MOR-ABIN-1-CHO cells treated with DAMGO (10 μM) for 0, 5, 30, and 60 minutes (A) or for 24, 36, or 48 hours (B). (C) Immunoblot analysis showing levels of MOR on plasma membrane of MOR-CHO and MOR-ABIN-1-CHO cells treated with DAMGO (10 μM) at 30 minutes or 72 hours of treatment. The error bars indicate the mean ± S.D., two-way ANOVA followed by Bonferroni post hoc test, $*P < 0.05$, $**P < 0.01$, $***P < 0.001$, ABIN-1 vs. vector at the same time; $\#\#\#\#P < 0.0001$, compared with 0 minutes in MOR-CHO cells, $n = 3–5$.

minutes: MOR-ABIN-1-CHO: $P < 0.0001$) or chronic (0 minutes: MOR-CHO vs. 72 hours: MOR-ABIN-1-CHO: $P < 0.0001$) DAMGO (10 μM) treatment. In contrast, MOR in the MOR-ABIN-1-CHO cell membrane did not decrease after DAMGO treatment of 30 minutes or 72 hours. The MOR in these two time points was higher than in the MOR-CHO cells at the same two time points (Fig. 3C). These data show that ABIN-1 inhibited the internalization of MOR after acute or chronic DAMGO exposure (30 minutes: MOR-CHO vs. 30 minutes: MOR-ABIN-1-CHO: $P = 0.0002$, 72 hours: MOR-

CHO vs. 72 hours: MOR-ABIN-1-CHO: $P = 0.0002$, F(1, 4) = 11.67, $P = 0.0269$; Fig. 3C). Along with the internalization of MOR, we also investigated the β-arrestin–related ERK activity in MOR-CHO and MOR-ABIN-1-CHO cells. Similar to MOR phosphorylation, ERK phosphorylation increased in MOR-CHO cells after 5-minute treatment with DAMGO (10 μM), with a time-dependent decrease in phosphorylation at 30 and 60 minutes. In MOR-ABIN-1-CHO cells, the increase in ERK phosphorylation attenuated after DAMGO (10 μM) treatment at 5, 30, and 60 minutes compared with MOR-CHO cells at these time points (0 minute: $P > 0.9999$, 5 minutes: $P = 0.0012$, 30 minutes: $P = 0.2667$, 60 minutes: $P = 0.0057$, F(1, 2) = 9.576, $P = 0.0905$; Fig. 3A). After 24 hours of DAMGO treatment, ERK phosphorylation was upregulated in MOR-CHO cells. In contrast, ERK phosphorylation was inhibited in MOR-ABIN-1-CHO cells after DAMGO treatment of 24 and 72 hours (0 minutes: $P = 0.4509$, 5 minutes: $P = 0.0035$, 24 hours: $P = 0.0084$, 48 hours: $P > 0.9999$, 72 hours: $P = 0.0136$, F(1, 2) = 43.23, $P = 0.0224$; Fig. 3B). These findings indicated ABIN-1 could regulate the β-arrestin–dependent pathway.

β-Arrestin2 Is Responsible for Morphine Tolerance Mediated by ABIN-1. Previous studies found that morphine tolerance was attenuated in ARRB2$^{-/-}$ mice (Bohn et al., 1999; Bohn et al., 2002; Lam et al., 2011). As we observed in the above experiments, the expression of β-arrestin2 is suppressed by interaction with ABIN-1; hence, we wanted to test whether β-arrestin2 is the key target of ABIN-1 to modulate morphine tolerance. Using ARRB2$^{-/-}$ mice, we provided intracerebroventricular injections of rAAV (PHPeB)-ABIN-1 or rAAV(PHPeB)-ABIN-1-shRNA [with rAAV(PHPeB)-vector injected in control group] to upregulate or downregulate ABIN-1, respectively. Wild-type (WT) mice were also used in the chronic morphine treatment test as another control. In the chronic morphine-induced tolerance test, the basal nociceptive latencies were similar in ARRB2$^{-/-}$ mice, with ABIN-1 overexpression or ARRB2$^{-/-}$ mice with ABIN-1 knockdown compared with these latencies in the control group (Fig. 4, A and B). Likewise, in ARRB2$^{-/-}$ mice in which ABIN-1 was overexpressed, the %MPE was the same as in the control group on days 1 to 7 of morphine treatment (10 mg/kg, s.c.) (WT vs. ARRB2$^{-/-}$ control: day 1: $P = 0.0025$, day 3: $P = 0.0001$, day 5: $P = 0.0596$, day 7: $P > 0.9999$, F(1, 4) = 46.92, $P = 0.0224$; ARRB2$^{-/-}$ control vs. ARRB2$^{-/-}$ ABIN-1: day 1: $P > 0.9999$, day 3: $P > 0.9999$, day 5: $P > 0.9999$, day 7: $P > 0.9999$, F(1, 4) = 0.005104, $P = 0.9465$; Fig. 4C). Similarly, the %MPE values did not change statistically as compared with the control group in the ARRB2$^{-/-}$ mice with downregulated ABIN-1 levels (WT vs. ARRB2$^{-/-}$ control: day 1: $P = 0.0014$, day 3: $P < 0.0001$, day 5: $P = 0.1188$, day 7: $P > 0.9999$, F(1, 5) = 23.75, $P = 0.0046$; ARRB2$^{-/-}$ control vs. ARRB2$^{-/-}$ sh-ABIN-1: day 1: $P > 0.9999$, day 3: $P > 0.9999$, day 5: $P > 0.9999$, day 7: $P > 0.9999$, F(1, 5) = 0.01734, $P = 0.9004$; Fig. 4D). These data suggested that ABIN-1 affected morphine tolerance through β-arrestin2.

Discussion

MOR is widely distributed in the mesolimbic dopamine circuitry and is involved in the modulation of pain and addiction (Serafini et al., 2020). Many opioid receptor–interacting proteins regulate the signal transduction pathways of MOR that modulate the effects of opioids (Georgoussi et al., 2012; Sakloth et al., 2020). In our previous study, the MOR-interacting protein Hsp90β was shown to positively regulate MOR function, and the Hsp90β inhibitor decreased the tolerance and dependence induced by morphine (Zhang et al., 2020). ABIN-1 is mainly expressed in human peripheral blood lymphocytes, the spleen, and skeletal muscle and plays an important role in regulating immunity (Nanda et al., 2011). However, few studies have investigated the role it plays in the nervous system. Our previous study confirmed that the association of ABIN-1 and MOR negatively regulated MOR function in CHO cells and zebrafish larvae (Zhou et al., 2018). In current study, we found that ABIN-1 modulated the behavioral response after morphine administration. Using adeno-associated virus, we first observed that ABIN-1 overexpression in the mouse brain attenuated morphine-induced tolerance and dependence. The effect of ABIN-1 on morphine tolerance was inhibited in β-arrestin2–deficient mice. This behavioral effect of ABIN-1 on morphine tolerance was associated with β-arrestin signaling via MOR. Indeed, our findings established ABIN-1 as a key regulator of morphine-mediated tolerance, providing keen insights into its functions (Fig. 1).

These behavioral effects of ABIN-1 on morphine dependence were detected by the hot-plate and CPP assay through adeno-associated virus injection into the cerebral ventricles. Although AAV(PHPeB) can efficiently pass through the blood-brain barrier, AAV(PHPeB)-ABIN-1-EGFP was not expressed in the whole brain by intracerebroventricular administration. As the AAV(PHPeB)-ABIN-1-EGFP has shown (Supp 1A), ABIN-1 and ABIN-1-shRNA were mainly expressed in the hippocampus. ABIN-1 in hippocampus might be involved in morphine tolerance and dependence. Previous studies have shown that the hippocampus contributes to morphine tolerance and withdrawal signs (Eitan et al., 2003; Koob and Volkow, 2010). Early studies showed that a partial hippocampectomy could treat chronic pain in humans (Jarrard and Lewis, 1967). Additionally, studies show that hippocampal formation can modify the processing of nociceptive information, including morphine-induced antinociception (Soleimannejad et al., 2006; Hashemi et al., 2010). Another recent study found that the ventral hippocampal CA1-infralimbic cortex modulates the progression of chronic pain in rats (Ma et al., 2019). Importantly, both MOR and ABIN-1 are widely expressed in the hippocampus (Ferreira-Chamorro et al., 2018), which suggests that they might interact with each other to play a role in hippocampal processing of pain sensations. Our results showed that the change of ABIN-1 expression in the mouse hippocampus modulated the antinociception and withdrawal behavior induced by morphine treatment. Thus, the hippocampus might be important for the effects of ABIN-1 on morphine function. Reward centers of the brain are related to morphine analgesia (Watanabe and Narita, 2018), and further research is needed to understand the effect of ABIN-1 on specific brain regions like Nac or anterior cingulate cortex in pain processing.

Studies have shown that ABINs act as ubiquitin adaptors (Zhou et al., 2011). In our study, we also found that the ABIN-1–β-arrestin2 complex could promote β-arrestin2 degradation by ubiquitination (Fig. 2). β-Arrestin2, as a multifunctional adaptor, mediates MOR trafficking and transduction to affect morphine tolerance. Downregulation of β-arrestin2 plays a

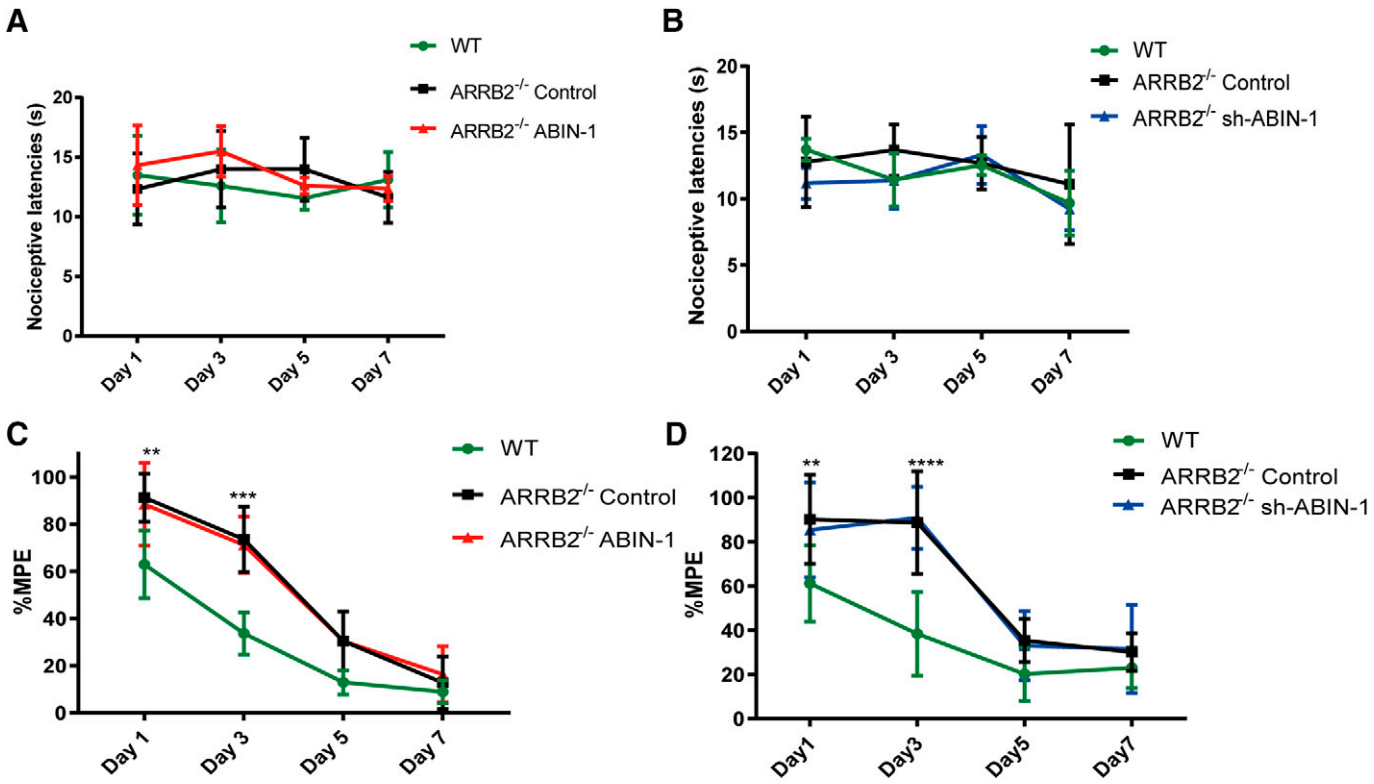

Fig. 4. β-Arrestin2 is responsible for the ABIN-1-induced reduction of morphine tolerance. (A and C) The nociceptive threshold (A) and %MPE of analgesia (C) induced by chronic morphine treatment in ARRB2$^{-/-}$ mice with ABIN-1 overexpression. (B, D) The nociceptive threshold (B) and %MPE of analgesia (D) induced by chronic morphine treatment in ARRB2$^{-/-}$ mice with ABIN-1 knockdown. The error bars indicate the mean ± S.D.; two-way ANOVA followed by Bonferroni post hoc test; ARRB2$^{-/-}$ control vs. WT; $^{*}P < 0.05$, $^{**}P < 0.01$, $^{***}P < 0.001$, $^{****}P < 0.0001$; n = 5–6.

vital role in MOR desensitization (Jean-Charles et al., 2016). MOR is phosphorylated and ubiquitinated and then follows arrestin-mediated internalization (Mittal and McMahon, 2009). Importantly, MOR activated by morphine only recruits β-arrestin2 (Groer et al., 2011). In the present study, we observed a notable reduction in MOR phosphorylation under acute or chronic MOR agonist treatment (Fig. 3, A and B). Two lines of evidence may explain why ABIN-1 decreased agonist-induced MOR phosphorylation. First, our previous work showed that ABIN-1 interacted with the MOR–C terminus, which has several phosphorylation sites. MOR phosphorylation is required for sustained interaction with GRKs under agonist activation (Inagaki et al., 2015). ABIN-1 may compete with GRKs to decrease MOR phosphorylation. Second, the ABIN-1–β-arrestin2–MOR complexes might produce strong steric hindrance to inhibit the function of GRKs. In mice with a series of serine and threonine to alanine mutants of MOR, the opioid-induced antinociception is enhanced, and analgesic tolerance is greatly inhibited, which further shows the phosphorylation-deficient MOR in mice inhibits antinociception tolerance induced by morphine (Kliewer et al., 2019). Our study shows that ABIN-1–mediated reduction of MOR phosphorylation and promoted β-arrestin2 degradation may likely be involved in modulating morphine tolerance.

β-arrestins regulate the internalization of many G protein—coupled receptors, including opioid receptors. It has been observed that both MOR phosphorylation and β-arrestin2 expression are related to MOR endocytosis. Specifically, the reduction of MOR phosphorylation and β-arrestin2 expression lead to a decrease in MOR internalization (Basso et al., 2019; Groer et al., 2011). In our study, higher ABIN-1 levels led to a decrease in β-arrestin2 levels and MOR phosphorylation. This

TABLE 1
Western blot antibodies

Antibody	Reagent Company	Reagent Number	Proportion
Anti-MOR	Millipore	Cat#AB1580- I	1:500
Anti–β-arrestin2	Life Spanbio Sciences	Cat#LS-B6008	1:1,000
Anti-FLAG M2	Sigma-Aldrich	F3165	1:5,000
Anti–ABIN-1	Cell Signaling Technology	Cat#4664	1:1,000
Anti-Myc	Cell Signaling Technology	Cat#2272	1:1,000
Anti–phos-MOR (Ser375)	Cell Signaling Technology	Cat#3451	1:1,000
Anti-ERK	Cell Signaling Technology	Cat#3857	1:1,000
Anti–phos-ERK	Cell Signaling Technology	Cat#9154	1:1,000
Anti–Na^+-K^+ATPase	Cell Signaling Technology	Cat#3010	1:1,000
Anti-UbP4D1	Santa Cruz Biotechnology Inc	Cat#sc-8017,	1:500
Anti-IgG	Santa Cruz Biotechnology Inc	Cat#sc-2025	1 μg

in turn inhibited internalization of MOR (Fig. 3C). Classic theory states that reduced MOR on the plasma membrane alters the normal signaling response to opioids, which in turn results in morphine tolerance. Thus, we found that ABIN-1 negatively regulated the β-arrestin signaling pathway, causing less internalization of MOR on the plasma membrane, which then attenuated morphine-induced tolerance.

β-Arrestins also act as scaffold-specific components of the mitogen-activated protein kinase (MAPK) cascade (Luttrell et al., 2001). Inhibition of the MAPK pathway blocks desensitization of MOR signaling and decreases the internalization of MOR (Polakiewicz et al., 1998). ERK1/2, members of the MAPK family, are crucial regulators of MOR signal transduction (Zheng et al., 2008). In our current study, we observed that ERK phosphorylation was inhibited by ABIN-1 under both acute and chronic morphine treatment (Fig. 3, A and B). As a downstream molecule in both the G protein– and β-arrestin–dependent pathways (Muller and Unterwald, 2004), the decrease in ERK activation by ABIN-1 is relevant to both pathways. In addition, ABIN-1 could act as an attenuator of activated ERK signaling by interaction with ERK (Zhang et al., 2002).

A previous study showed that morphine tolerance is reversed and the severity of antagonist-precipitated withdrawal signs is attenuated after chronic morphine exposure in β-arrestin2–knockout mice (Bohn et al., 2002; Raehal and Bohn, 2011; Wang et al., 2016). These studies have shown that β-arrestin2 plays an important role in morphine tolerance and dependence. In our study, ABIN-1 had no effect on morphine tolerance in β-arrestin2–knockout mice (Fig. 4), which suggests that ABIN-1 may alleviate morphine tolerance through downregulation of β-arrestin2 expression. Additionally, it has been reported that A20, the interacting protein of ABIN-1, attenuated morphine tolerance (Huang et al., 2019) and enhanced MOR function by inhibiting β-arrestin2 recruitment (Shao et al., 2020). Therefore, ABIN-1 and A20 may work together to participate in mediating morphine tolerance.

In summary, we found that the ABIN-1–β-arrestin2 complex functionally diminished MOR phosphorylation and β-arrestin2 expression, which led to a reduction in MOR internalization. Through this mechanism, ABIN-1 overexpression in the mouse brain alleviated morphine tolerance and dependence. This finding was further confirmed by our observation that the therapeutic effect of ABIN-1 on morphine tolerance was blocked in β-arrestin2–knockout mice. Overall, we found that ABIN-1 attenuated morphine-induced tolerance and dependence, which is an important finding that can be used as a potential strategy to improve the therapeutic profile of opioids.

Acknowledgments

We would like to give our sincere appreciation to the National Natural Science Foundation (81473194) for their financial help. We would like to thank Accdon (www.accdon.com) for providing linguistic assistance during the preparation of this manuscript.

Authorship Contributions

Participated in research design: Zhou, Su, Gong.

Conducting experiments: Zhang, Lu.

Contributed new reagents or analytic tools: Zhou, Su.

Performed data analysis: Zhang, Zhou.

Wrote or contributed to the writing of the manuscript: Zhang, Zhou, Su.

References

Allouche S, Noble F, and Marie N (2014) Opioid receptor desensitization: mechanisms and its link to tolerance. *Front Pharmacol* **5**:280.

Attramadal H, Arriza JL, Aoki C, Dawson TM, Codina J, Kwatra MM, Snyder SH, Caron MG, and Lefkowitz RJ (1992) Beta-arrestin2, a novel member of the arrestin/beta-arrestin gene family. *J Biol Chem* **267**:17882–17890.

Basso L, Aboushousha R, Fan CY, Iftinca M, Melo H, Flynn R, Agosti F, Hollenberg MD, Thompson R, Bourinet E, et al. (2019) TRPV1 promotes opioid analgesia during inflammation. *Sci Signal* **12**:eaav0711.

Bohn LM, Gainetdinov RR, Lin FT, Lefkowitz RJ, and Caron MG (2000) Mu-opioid receptor desensitization by beta-arrestin-2 determines morphine tolerance but not dependence. *Nature* **408**:720–723.

Bohn L, Lefkowitz R, and Caron MG (2002) Differential mechanisms of morphine antinociceptive tolerance revealed in (beta)arrestin-2 knock-out mice. *J Neurosci* **22**:10494–10500.

Bohn LM, Lefkowitz RJ, Gainetdinov RR, Peppel K, Caron MG, and Lin FT (1999) Enhanced morphine analgesia in mice lacking beta-arrestin 2. *Science* **286**:2495–2498.

Eddy NB and Leimbach D (1953) Synthetic analgesics. II. Dithienylbutenyl- and dithienylbutylamines. *J Pharmacol Exp Ther* **107**:385–393.

Eitan S, Bryant CD, Saliminejad N, Yang YC, Vojdani E, Keith Jr D, Polakiewicz R, and Evans CJ (2003) Brain region-specific mechanisms for acute morphine-induced mitogen-activated protein kinase modulation and distinct patterns of activation during analgesic tolerance and locomotor sensitization. *J Neurosci* **23**:8360–8369.

el-Kadi AO and Sharif SI (1994) The influence of various experimental conditions on the expression of naloxone-induced withdrawal symptoms in mice. *Gen Pharmacol* **25**:1505–1510.

Ferreira-Chamorro P, Redondo A, Riego G, Leánez S, and Pol O (2018) Sulforaphane inhibited the nociceptive responses, anxiety- and depressive-like behaviors associated with neuropathic pain and improved the anti-allodynic effects of morphine in mice. *Front Pharmacol* **9**:1332.

Georgoussi Z, Georganta EM, and Milligan G (2012) The other side of opioid receptor signalling: regulation by protein-protein interaction. *Curr Drug Targets* **13**:80–102.

Groer CE, Schmid CL, Jaeger AM, and Bohn LM (2011) Agonist-directed interactions with specific beta-arrestins determine mu-opioid receptor trafficking, ubiquitination, and dephosphorylation. *J Biol Chem* **286**:31731–31741.

Hashemi M, Karami M, Zarrindast MR, and Sahebgharani M (2010) Role of nitric oxide in the rat hippocampal CA1 in morphine antinociception. *Brain Res* **1313**:79–88.

Heyninck K, Kreike MM, and Beyaert R (2003) Structure-function analysis of the A20-binding inhibitor of NF-κ B activation, ABIN-1. *FEBS Lett* **536**:135–140.

Huang J, Liang X, Wang J, Kong Y, Zhang Z, Ding Z, Song Z, Guo Q, and Zou W (2019) miR-873a-5p targets A20 to facilitate morphine tolerance in mice. *Front Neurosci* **13**:347.

Inagaki S, Ghirlando R, Vishnivetskiy SA, Homan KT, White JF, Tesmer JJ, Gurevich VV, and Grisshammer R (2015) G protein-coupled receptor kinase 2 (GRK2) and 5 (GRK5) exhibit selective phosphorylation of the neurotensin receptor in vitro. *Biochemistry* **54**:4320–4329.

Jarrard LE and Lewis TC (1967) Effects of hippocampal ablation and intertrial interval on acquisition and extinction in a complex maze. *Am J Psychol* **80**:66–72.

Jean-Charles PY, Freedman NJ, and Shenoy SK (2016) Chapter nine - cellular roles of beta-arrestins as substrates and adaptors of ubiquitination and deubiquitination. *Prog Mol Biol Transl Sci* **141**:339–369.

Kliewer A, Schmiedel F, Sianati S, Bailey A, Bateman JT, Levitt ES, Williams JT, Christie MJ, and Schulz S (2019) Phosphorylation-deficient G-protein-biased μ-opioid receptors improve analgesia and diminish tolerance but worsen opioid side effects. *Nat Commun* **10**:367.

Koob GF and Volkow ND (2010) Neurocircuitry of addiction. *Neuropsychopharmacology* **35**:217–238.

Koshimizu TA, Honda K, Nagaoka-Uozumi S, Ichimura A, Kimura I, Nakaya M, Sakai N, Shibata K, Ushijima K, Fujimura A, et al. (2018) Complex formation between the vasopressin 1b receptor, β-arrestin-2, and the μ-opioid receptor underlies morphine tolerance. *Nat Neurosci* **21**:820–833.

Lam H, Maga M, Pradhan A, Evans C, Maidment N, Hales T, and Walwyn W (2011) Analgesic tone conferred by constitutively active mu opioid receptors in mice lacking β-arrestin 2. *Mol Pain* **7**:24.

Le Rouzic V, Narayan A, Hunkle A, Marrone GF, Lu Z, Majumdar S, Xu J, Pan YX, and Pasternak GW (2019) Pharmacological characterization of levorphanol, a G-protein biased opioid analgesic. *Anesth Analg* **128**:365–373.

Li Y, Liu X, Liu C, Kang J, Yang J, Pei G, and Wu C (2009) Improvement of morphine-mediated analgesia by inhibition of β-arrestin2 expression in mice periaqueductal gray matter. *Int J Mol Sci* **10**:954–963.

Lu GY, Wu N, Zhang ZL, Ai J, and Li J (2011) Effects of D-cycloserine on extinction and reinstatement of morphine-induced conditioned place preference. *Neurosci Lett* **503**:196–199.

Luttrell LM, Roudabush FL, Choy EW, Miller WE, Field ME, Pierce KL, and Lefkowitz RJ (2001) Activation and targeting of extracellular signal-regulated kinases by beta-arrestin scaffolds. *Proc Natl Acad Sci USA* **98**:2449–2454.

Ma L, Yue L, Zhang Y, Wang Y, Han B, Cui S, Liu FY, Wan Y, and Yi M (2019) Spontaneous pain disrupts ventral hippocampal CA1-infralimbic cortex connectivity and modulates pain progression in rats with peripheral inflammation. *Cell Rep* **29**:1579–1593.e6.

Manglik A, Lin H, Aryal DK, McCorvy JD, Dengler D, Corder G, Levit A, Kling RC, Bernat V, Hübner H, et al. (2016) Structure-based discovery of opioid analgesics with reduced side effects. *Nature* **537**:185–190.

Mittal R and McMahon HT (2009) Arrestins as adaptors for ubiquitination in endocytosis and sorting. *EMBO Rep* **10**:41–43.

Muller DL and Unterwald EM (2004) In vivo regulation of extracellular signal-regulated protein kinase (ERK) and protein kinase B (Akt) phosphorylation by acute and chronic morphine. *J Pharmacol Exp Ther* **310**:774–782.

Nanda SK, Venigalla RK, Ordureau A, Patterson-Kane JC, Powell DW, Toth R, Arthur JS, and Cohen P (2011) Polyubiquitin binding to ABIN1 is required to prevent autoimmunity. *J Exp Med* **208**:1215–1228.

Polakiewicz RD, Schieferl SM, Dorner LF, Kansra V, and Comb MJ (1998) A mitogen-activated protein kinase pathway is required for μ-opioid receptor desensitization. *J Biol Chem* **273**:12402–12406.

Raehal KM and Bohn LM (2011) The role of beta-arrestin2 in the severity of antinociceptive tolerance and physical dependence induced by different opioid pain therapeutics. *Neuropharmacology* **60**:58–65.

Sadat-Shirazi MS, Monfared Neirizi N, Matloob M, Safarzadeh M, Behrouzi M, Rajabpoor Dehdashti A, Ashabi G, and Zarrindast MR (2019) Possible involvement of nucleus accumbens D1-like dopamine receptors in the morphine-induced condition place preference in the offspring of morphine abstinent rats. *Life Sci* **233**:116712.

Sakloth F, Polizu C, Bertherat F, and Zachariou V (2020) Regulators of G protein signaling in analgesia and addiction. *Mol Pharmacol* **98**:739–750.

Schulz S, Mayer D, Pfeiffer M, Stumm R, Koch T, and Höllt V (2004) Morphine induces terminal micro-opioid receptor desensitization by sustained phosphorylation of serine-375. *EMBO J* **23**:3282–3289.

Serafini RA, Pryce KD, and Zachariou V (2020) The mesolimbic dopamine system in chronic pain and associated affective comorbidities. *Biol Psychiatry* **87**:64–73.

Shao S, Sun Y, Zhang Y, Tian X, Li Y, Tan B, and Su R (2020) A20 enhances mu-opioid receptor function by inhibiting beta-arrestin2 recruitment. *Biochem Biophys Res Commun* **528**:127–133.

Sharma SK KWA, Nirenberg M. (1975) Dual regulation of adenylate cyclase accounts for narcotic dependence and tolerance. *Proceedings of the National Academy of Sciences*, **72**(8): 3092–3096.

Shukla AK, Xiao K, and Lefkowitz RJ (2011) Emerging paradigms of β-arrestin-dependent seven transmembrane receptor signaling. *Trends Biochem Sci* **36**:457–469.

Soleimannejad E, Semnanian S, Fathollahi Y, and Naghdi N (2006) Microinjection of ritanserin into the dorsal hippocampal CA1 and dentate gyrus decrease nociceptive behavior in adult male rat. *Behav Brain Res* **168**:221–225.

Takenouchi O, Yoshimura H, and Ozawa T (2018) Unique roles of β-arrestin in GPCR trafficking revealed by photoinducible dimerizers. *Sci Rep* **8**:677.

Wang J, Xu W, Zhong T, Song Z, Zou Y, Ding Z, Guo Q, Dong X, and Zou W (2016) miR-365 targets β-arrestin 2 to reverse morphine tolerance in rats. *Sci Rep* **6**:38285.

Wang XY, Zhao M, Ghitza UE, Li YQ, and Lu L (2008) Stress impairs reconsolidation of drug memory via glucocorticoid receptors in the basolateral amygdala. *J Neurosci* **28**:5602–5610.

Watanabe M and Narita M (2018) Brain reward circuit and pain. *Adv Exp Med Biol* **1099**:201–210.

Whalen EJ, Rajagopal S, and Lefkowitz RJ (2011) Therapeutic potential of β-arrestin- and G protein-biased agonists. *Trends Mol Med* **17**:126–139.

Williams JT, Ingram SL, Henderson G, Chavkin C, von Zastrow M, Schulz S, Koch T, Evans CJ, and Christie MJ (2013) Regulation of μ-opioid receptors: desensitization, phosphorylation, internalization, and tolerance. *Pharmacol Rev* **65**:223–254.

Wu XP, She RX, Yang YP, Xing ZM, Chen HW, and Zhang YW (2018) MicroRNA-365 alleviates morphine analgesic tolerance via the inactivation of the ERK/CREB signaling pathway by negatively targeting β-arrestin2. *J Biomed Sci* **25**:10.

Zhang S, Fukushi M, Hashimoto S, Gao C, Huang L, Fukuyo Y, Nakajima T, Amagasa T, Enomoto S, Koike K, et al. (2002) A new ERK2 binding protein, Naf1, attenuates the EGF/ERK2 nuclear signaling. *Biochem Biophys Res Commun* **297**:17–23.

Zhang Y, Zhou P, Wang Z, Chen M, Fu F, and Su R (2020) Hsp90β positively regulates μ-opioid receptor function. *Life Sci* **252**:117676.

Zheng H, Loh HH, and Law PY (2008) Beta-arrestin-dependent mu-opioid receptor-activated extracellular signal-regulated kinases (ERKs) Translocate to Nucleus in Contrast to G protein-dependent ERK activation. *Mol Pharmacol* **73**:178–190.

Zhou J, Wu R, High AA, Slaughter CA, Finkelstein D, Rehg JE, et al. (2011) A20-binding inhibitor of NF- B (ABIN1) controls Toll-like receptor-mediated CCAAT/enhancer-binding protein activation and protects from inflammatory disease. *Proc Natl Acad Sci USA* **108**:998–1006.

Zhou P, Jiang J, Dong Z, Yan H, You Z, Su R, and Gong Z (2015) The proteins interacting with C-terminal of μ receptor are identified by bacterial two-hybrid system from brain cDNA library in morphine-dependent rats. *Life Sci* **143**:156–167.

Zhou P, Jiang J, Yan H, Li Y, Zhao J, Wang X, Su R, and Gong Z (2018) ABIN-1 negatively regulates μ-opioid receptor function. *Mol Pharmacol* **93**:36–48.

Address correspondence to: Ruibin Su, State Key Laboratory of Toxicology and Medical Countermeasures, Beijing Key Laboratory of Neuropsychopharmacology, Beijing Institute of Pharmacology and Toxicology, 27th Taiping Rd., Beijing 100850, China. E-mail: ruibinsu@126.com; or Peilan Zhou, State Key Laboratory of Toxicology and Medical Countermeasures, Beijing Key Laboratory of Neuropsychopharmacology, Beijing Institute of Pharmacology and Toxicology, 27th Taiping Rd., Beijing 100850, China. E-mail: zhoupeilan0502@sina.com

ABIN-1 targets β-arrestin-2 to attenuate opioid tolerance

Yixin Zhang, Peilan Zhou*, Fengfeng Lu, Ruibin Su*, Zehui Gong

MOLPHARM-AR-2020-000211R4

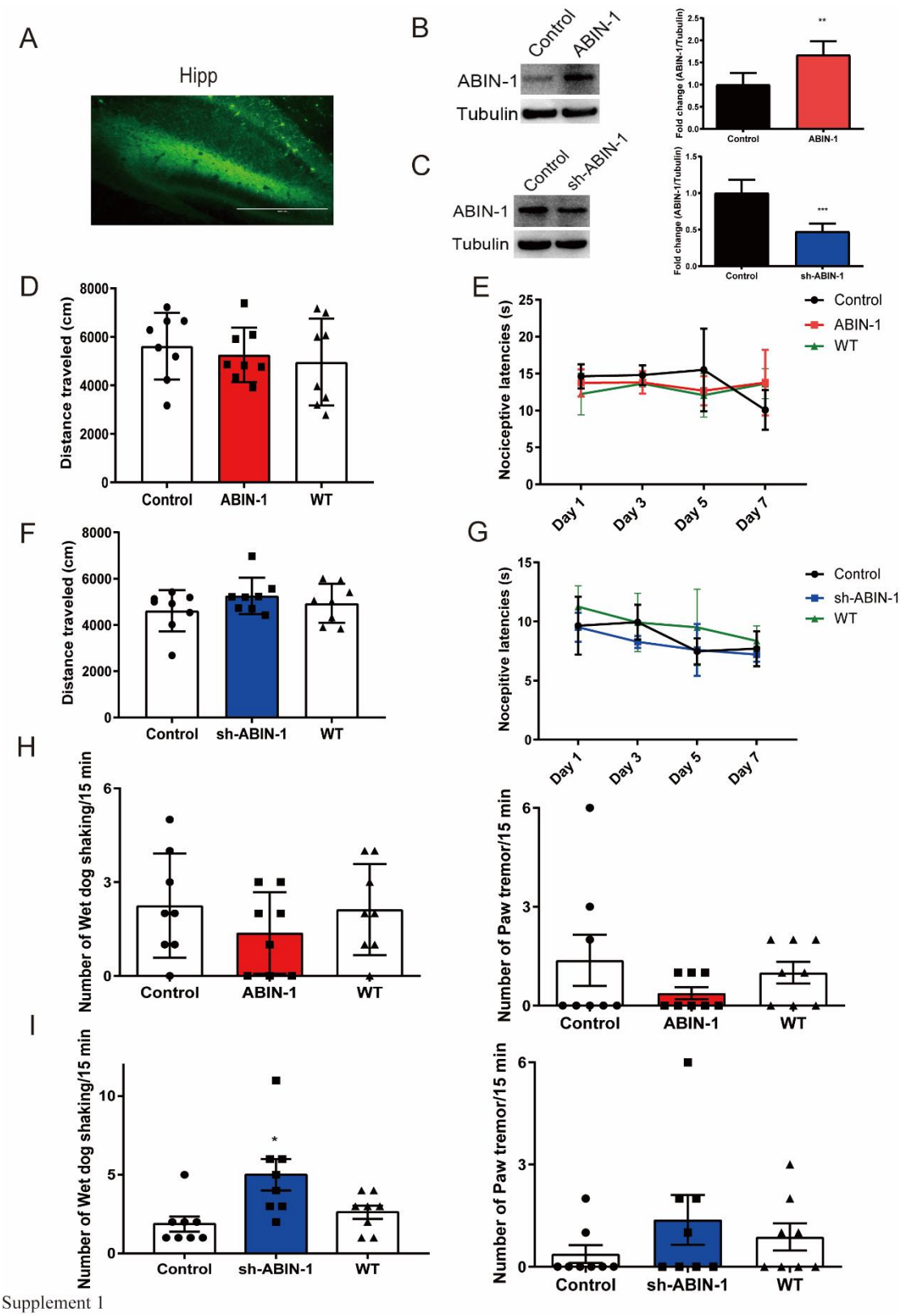

Supplement 1

Supplementary1. The nociceptive latencies and locomotor behaviour of mice prior to morphine treatment. (A) EGFP-labelled neurons in the hippocampus

following i.c.v. injection with AAV-ABIN-1-virus, bar: 200 μm. (B-C) Immunoblotting analysis and quantification of ABIN-1 levels in brain tissue of mice with i.c.v. injection of AAV(PHPeB)-ABIN-1 (B) and AAV(PHPeB)-ABIN-1-shRNA (C), n=5. (D-E) The locomotor behaviour (D) and nociceptive latency (E) in mice with overexpression of ABIN-1. (F-G) The locomotor behaviour (F) and nociceptive latency (G) in mice with ABIN-1 knockdown. (H) Wet dog shaking (left) and paw tremors (right) in mice with ABIN-1 overexpression. (I) Wet dog shaking (left) and paw tremors (right) in mice with ABIN-1 knockdown. The error bars indicate the means ± SD; behaviour test results were analysed by two-way ANOVA followed by Bonferroni post hoc test; immunoblot results were analysed by Student's t test; ABIN-1 vs control, $*P < 0.05$, $**P < 0.01$, $***P < 0.001$, hotplate assay used female mice, n = 8; withdrawal assay used female mice, n=8.

ABIN-1 targets β-arrestin-2 to attenuate opioid tolerance

Yixin Zhang, Peilan Zhou*, Fengfeng Lu, Ruibin Su*, Zehui Gong

MOLPHARM-AR-2020-000211R4

A

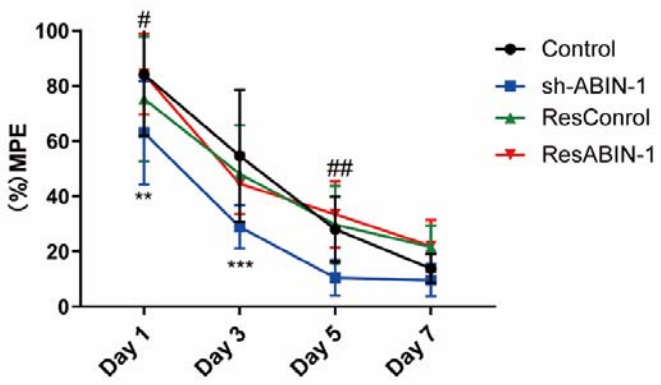

B

Table2 95% CI of difference of figure

Figure	95% CI of difference
Figure1 B	-25.90 to -14.49
Figure1 C	3.805 to 50.70
Figure1 E(Baseline control vs Post-c contol)	-317.0 to -6.320
Figure1 E(Post-c control vs Post-c ABIN-1)	21.32 to 299.5
Figure1 F	7.082 to 27.82
Figure1 G	-32.63 to -5.373
Figure1 H(Baseline control vs Post-c contol)	-400.4 to -16.68
Figure1 E(Post-c control vs Post-c shABIN-1)	-279.1 to -16.94
Figure2 D	-0.5397 to -0.1313
Figure2 E	0.2234 to 0.5697
Figure3 A phos MOR	-0.05059 to 0.4152
Figure3 A phos ERK	-0.1104 to 0.6763
Figure3 B phos MOR	0.1000 to 0.4750
Figure3 B phos ERK	0.08034 to 0.3846
Figure3 C	-0.5342 to -0.05521
Figure4 C	-31.47 to -13.32
Figure4 D	-38.81 to -12.01
Supplement 2A	-30.17 to -6.019

Supplement 2

Supplementary2. The hot plate test results of reversing ABIN-1 in ABIN-1 knockdown mice and the table of 95% confidence interval (CI) of difference

figure. The error bars indicate the means ± SD; behaviour test results were analysed by two-way ANOVA followed by Bonferroni post hoc test; sh-ABIN-1 vs control, *$P < 0.05$, **$P < 0.01$, ***$P < 0.001$, sh-ABIN-1 vs ResABIN-1, #$P < 0.05$, ##$P < 0.01$, hotplate assay used female mice, n = 8.